Electronics Research Laboratory
University of California
Berkeley, California
Internal Technical Memorandum M-84

LASER INDUCED EMISSION OF ELECTRONS, IONS, AND NEUTRALS FROM Ti AND Ti-D SURFACES*

by

T. Y. Chang

* The research herein was supported by the Joint Services Electronics Program (Air Force Office of Scientific Research, Army Research Office, Office of Naval Research) under Grant AF-AFOSR-139-63 and AF-AFOSR-139-64.

July 28, 1964

I. INTRODUCTION

Deuterium loaded titanium discs are often used in plasma guns as deuterium reservoirs. The lack of knowledge of physical processes involved in the production of plasma in such a gun, however, makes the control of the gun very difficult. It is, therefore, of great importance to know the mechanism or mechanisms by which deuterium plasmas are produced from Ti-D discs, in order to design a more manageable plasma gun. This experimental investigation was originally intended for such purposes. The information obtained from this investigation, although of limited value to the original purposes, is of quite general interest in the field of laser-solid interactions. The results we obtained agree in general with other published works.[1-7] We particularly discuss the blow-off mechanism which is postulated as responsible for the production of high-energy ions.

II. DESCRIPTION OF THE APPARATUS

A ruby laser rated at one joule output was used throughout our experiments. The actual output power was not measured. The laser beam is focused by a lens with two-inch focal length onto the target surface. The target is a circular disc 1/2 inch in diameter and 1/16 inch in thickness. It is mounted inside a vacuum system which is maintained at 10^{-7} Torr. A molybdenum collector is mounted in front of the target with 1/4 inch separation. The collector is one inch x one inch in dimension and has a 1/4 inch hole at its center. The target and the collector are connected to a circuit as shown in Fig. 1. The bias voltage can be varied from -30 volts to +30 volts. The load resistor varies from 10^5 ohms to 2.7 ohms depending on the peak current.

The relative intensity of the laser beam is monitored by an RCA 925 photo-tube. The photo-tube picks up the laser light scattered from the lens surface. The diode current and the photo-tube current are displayed simultaneously on a dual-beam scope.

III. EXPERIMENTAL RESULTS

The results of five experiments with different combinations of target material and laser power are summarized in Table I.

The Ti-D target was prepared by heating a titanium disc in a deuterium atmosphere. The degree of occlusion is estimated to be about one deuterium atom per two titanium atoms.

The laser power is only an approximate estimation from the rated value. The spot size for the focused laser beam is estimated from the size of the craters created by the laser in experiments III and V. Again this is only approximate.

In experiments I, II and III, the amplitudes of the current pulses and the corresponding laser pulses are not well correlated. The values given in Table I are the maximum peak values recorded by the photographic plates. In experiments II and III, the emission seems to depend strongly on the existence of a monolayer on the target surface. Repeated bombardments of the same spot tends to clean up the surface. The high current values tabulated are obtained before the surface is cleaned up. The low current values are obtained after the surface is cleaned up.

In experiment V, the electron current pulses break into a continuous discharge current for bias voltages above +20 volts. The duration of the discharge increases both with the laser peak power and the bias voltage. It is from 27 μsec to over 100 μsec at +30 volts bias. The discharge always ceases very abruptly.

The numbers of electrons and ions collected are obtained by integrating the current of the largest pulses recorded at the specified bias voltages. Fig. 2 shows the plot of the number of electrons per pulse versus the electron-retarding bias voltage in experiments IV and V

TABLE I

Experiment	I	II	III	IV	V
Target	Ti-D	Ti	Ti	Ti-D	Ti-D
Laser type	non-Q-switched			Q-switched	
power (Kw)	~1	~1	~10	~100	~100
spot size (cm^2)	$\sim 10^{-3}$	$\sim 10^{-3}$	$\sim 10^{-3}$	~0.3	$\sim 10^{-3}$
pwr density (w/cm^2)	$\sim 10^{6}$	$\sim 10^{6}$	$\sim 10^{7}$	$\sim 10^{5}$	$\sim 10^{8}$
Bias (volts)	peak electron current				
30	30 uA	50→ 2 uA	100→ 3uA	——	4.5A discharge
20	——	——	——	——	3.3 A
10	10 uA	——	——	——	2.4 A (at 12v)
0	6 uA	——	——	0.8 uA	0.40 A
-2	0.5 uA	——	——	0.2 uA	0.25 A
	peak ion current				
0	0	——	——	0	0.02 A
-3	0.9 uA	——	——	0.7 uA(-4v)	0.15 A
-30	1.7 uA	0.1 uA	10 → 0.5 uA	——	5.6 A
Electrons collected per pulse	4×10^{8} max w. 30v bias	——	——	1.1×10^{7} w/no bias	1.5×10^{13} w/10v bias
Ions collected per pulse	4×10^{7} max w/-30v bias	——	——	2.3×10^{7} w/-4v bias	6.3×10^{13} w/-30v bias
Te (°K) from retarding potential plot				7000	16,600
Temperature (°K)	total thermionic current (Amp.)				
900	3.5×10^{-18}	3.5×10^{-18}	3.5×10^{-18}	1.0×10^{-15}	3.5×10^{-18}
1200	2.5×10^{-12}	2.5×10^{-12}	2.5×10^{-12}	7.7×10^{-10}	2.5×10^{-12}
1500	9.3×10^{-9}	9.3×10^{-9}	9.3×10^{-9}	2.8×10^{-6}	9.3×10^{-9}
1800	2.3×10^{-6}	2.3×10^{-6}	2.3×10^{-6}	7.0×10^{-4}	2.3×10^{-6}
2100	1.3×10^{-4}	1.3×10^{-4}	1.3×10^{-4}	3.8×10^{-2}	1.3×10^{-4}
2400	2.5×10^{-3}	2.5×10^{-3}	2.5×10^{-3}	0.79	2.5×10^{-3}
2700	2.9×10^{-2}	2.9×10^{-2}	2.9×10^{-2}	8.7	2.9×10^{-2}
3000					0.2
Approximate temperature rise from heat flow equation.					
$T-T_o$ (°K)	340	340	3400	34	34,000

and the corresponding temperature. In experiment V, about 10^{15} neutrals are lifted off the surface per pulse, as calculated from the crater size and the pressure rise.

The total thermionic currents, as a function of temperature, are tabulated for reference. These are calculated from the Richardson-Dushman equation using $\phi = 4.0$ volts, and the estimated spot size.

An estimation of the peak surface temperature can be obtained from the following expression, which is the solution of heat flow equation for a semi-infinite conductor with constant heat flux input.

$$T - T_o = \sqrt{\frac{2}{\pi K \rho c}} \quad \frac{W}{A} \quad \alpha \sqrt{\tau}$$

Here, T is in degrees Kelvin, W is the laser power in watts, A is the target area in cm^2, α is the absorptivity of the surface, τ is the duration of the laser pulse; ρ, K, c are the density, thermal conductivity and specific heat, respectively. Using the wave equation, we get the root = 2.27 and $\alpha = 0.15$ for Ti at the frequency of the ruby laser. The last row in Table I gives the temperature rise calculated from the above expression for $\tau = 10^{-6}$ sec. The values of all parameters are only approximate and no temperature dependence of the parameters has been taken into account. Of course, such a roughly estimated temperature cannot be used to estimate even the order of magnitude of the thermionic current. However, it gives us some ideas about the attainable surface temperature in different experiments.

Figs. 3 through 26 show the oscilloscope traces obtained under various conditions.

IV. DISCUSSION OF THE RESULTS

A. ELECTRON CURRENTS

There are four possible mechanisms by which electrons can be produced, namely, (a) photoelectric effects, (b) thermionic emission, (c) thermal ionization, (d) gaseous breakdown. The first mechanism is unimportant for laser photons, since the photon energy is only 1.79 eV, while the work function of Ti is about 4.0 eV. The fourth mechanism is important only when a discharge occurs in the diode. The third mechanism is important when the laser pulse evaporates a large number of particles from the target surface and the number of ions collected is comparable to the number of electrons collected. In many cases, the number of ions collected is much smaller than the number of electrons collected. The electron emission is then chiefly thermionic in nature.

When thermionic emission is prevalent, the emission current density is given by Richardson-Dushman equation,

$$J_{th} = A_o T^2 \exp(-e\phi/KT) \tag{1}$$

where A_o is a constant. The total current is given by integration of J_{th} over the emission area. If one knows the effective emission area, then he can calculate the effective temperature from this equation. Unfortunately, since J_{th} is a nonlinear function of T, an effective emission area cannot be defined unless the temperature distribution on the targer surface is completely known. Using the approximate cross-section of the laser beam at the target surface as the effective emission area often leads to an unreasonable result.

The electron temperature can, however, be more reliably determined by plotting the number of electrons collected versus the retarding potential applied, assuming, of course, a half Maxwellian distribution for the electrons. This method gives us an electron temperature of 7000°K in experiment IV, and 16, 600°K in experiment V.

The electron temperature in experiment IV is surprisingly high, since the heat flow calculation predicts a temperature rise of only 34°C. The high temperature is also incompatible with the small emission current. This can be explained only if the temperature distribution on the target surface is extremely peaked at one or more small spots. Because of the nonlinearity of Richardson-Dushman equation, the electrons will come almost exclusively from these hottest spots.

In experiment V, the input power density is increased by about three orders of magnitude by focusing. This causes the electron temperature to increase by a factor of a little more than two, and the electron current to increase by about six orders of magnitude. The temperature rise is presumably limited by a large specific heat at high temperatures and the increased transparency of the material due to expansion.

In experiments I, II and III the electron current exhibits extremely large fluctuations from pulse to pulse. This prevents us from determining the electron temperatures through retarding potential plots. The large fluctuations of the electron current is understandable as a ten percent change in temperature could cause a ten fold change in the thermionic current density. This kind of fluctuation is remarkably small in experiment IV, presumably due to the large illuminated area.

The cleaning-up effect observed in experiments II and III implies that the presence of a monolayer on the target surface reduces the work function by about ten percent. Comparison of data between experiments I and II indicates that the occlusion of deuterium particles has a similar effect as the presence of a monolayer.

B. ION CURRENTS

Possible mechanisms of ion production are (a) direct emission from the solid surface, (b) thermal ionization in the evaporated gas, (c) surface ionization of vapor molecules at the target surface, (d) field intensified ionization in the evaporated gas. The last mechanism is important when there is a discharge in the diode. The second mechanism is governed by Saha equation; the third, by Langmuir-Saha equation. The first mechanism is not well understood. Our experimental data are not sufficient to determine the relative importance of different mechanisms in various cases. Consequently, we are not able to estimate the ion temperature from the ion current we observed. We could not determine the ion temperature by retarding potential plot as we did for the electrons, because the ion current was practically not observable when a retarding potential is applied.

To extract useful information from the pulse shape of ion current induced in the external circuit, it is necessary first to consider the relations between current in the circuit and ion flow in the diode.

We consider first the situations in experiment IV. The low power, low density, and low current in this experiment allow us to neglect the space charge and collisions in the diode and the change of voltage across the diode. We also assume that the ion thermal energies are small compared to the potential energy across the diode so that the ions can be treated as emitted with zero initial velocity at the target surface. Because of lack of better information, we assume the ion emission current to decay exponentially with time. The e-folding time of decay is four microseconds, as determined from the tail of actual ion current pulses.

The distribution of ions in the diode must satisfy the continuity equation

$$\frac{\partial}{\partial t} n + \frac{\partial}{\partial x} (nu) = 0 \qquad (2)$$

where n is the number of ions per unit distance, u is the flow velocity of ions in the x direction.

The equation of motion must also be satisfied,

$$\frac{\partial}{\partial t} u + u \frac{\partial}{\partial x} u = \frac{e}{m} E \quad . \tag{3}$$

E is the applied electric field. Since the bias voltage is nearly constant,

$$E = \frac{V}{d} = \text{const.} \tag{4}$$

The solution of (3) with the boundary condition $u = 0$ at $x = 0$ is

$$u = (2e\,Ex/m)^{1/2}. \tag{5}$$

Using Eqs. (2), (3), and (5), we can obtain the following equation for convection current $J = en\,u$,

$$\frac{\partial}{\partial t} J + (2e\,Ex/m)^{1/2} \frac{\partial}{\partial x} J = 0 \, . \tag{6}$$

The solution of (6) satisfying the boundary condition $J = J_o \exp(-t/\tau)$ is

$$J = J_o \exp \left[(1/\tau)(2m/xeE)^{1/2} - (t/\tau)\right] \quad . \tag{7}$$

If both D^+ and Ti^+ are present, the total convection current is given by $J = J_D + J_T$. The total power input to the diode is equal to

$$P = VI = \int_o^d JE\,dx = \frac{V}{d} \int_o^d J dx$$

or

$$I = I_D + I_T = \frac{1}{d}\int_o^d (J_D + J_T)\, dx \quad . \tag{8}$$

Using Eq. (7), we have

$$\begin{aligned} I_D &= J_{Do} \exp(-t/\tau) \int_o^d \exp\left((2m_D x/eE)^{1/2}/\tau\right) dx \\ &= 2J_{Do}(\tau/t_o)^2 \left[1 - (1 - (t_D/\tau)) \exp(t_D/\tau)\right] \exp(-t/\tau) \end{aligned} \tag{9}$$

where $t_D = (2dm_D/eE)^{1/2}$ is the transit time of a D_2^+ ion. Eq. (9) holds only for $t \geq t_D$. For $0 < t < t_D$, the diode is only partly filled with ions. The upper limit of the integral should be replaced by $x = (eE/2m_D)t^2$. The result is

$$\begin{aligned} I_D &= 2J_{Do}(\tau/t_D)^2 \left[\exp(-t/\tau) - 1 + (t/\tau)\right] \\ &\approx J_{Do}(t/t_D)^2 \qquad \text{for } t << \tau \ . \end{aligned} \tag{10}$$

I_T is the same as I_D except that J_{Do} and m_D must be replaced by J_{To} and m_T.

I is plotted for the case of V = 4 volts, τ = 4 microseconds, J_{Do} = 0.7 microamp, J_{To} = 0.5 microamp, and d = 1.0 cm,* in Fig. 27. The result is in good agreement with the experimental pulse form shown in Fig. 18.

---

* The actual collector to target distance is 0.64 cm. We use an effective distance of one cm because there is a 1/4 inch hole in the front of the target.

The above calculation reveals that if there is only one species of ions the total rise time of the ion-current pulse is equal to the diode transit time of an ion. When we apply this result to experiment III, in which the peak ion current is also less than one microamp, we find that the assumption of zero initial velocity is not satisfied, because the ion-current rise time does not follow the $V^{-1/2}$ law. To fit the experimental data, we now have to assume a non-zero initial velocity for ions.

Let V_o be the voltage corresponding to the initial energy of an ion. Then, the ion transit time is given by

$$t_j = (2md^2/e)^{1/2} \Big/ \left[(V_o + V_j)^{1/2} + V_o^{1/2}\right] . \qquad (11)$$

The ratio of transit times for two different bias voltages is

$$t_1/t_2 = \left[(V_o + V_2)^{1/2} + V_o^{1/2}\right] \Big/ \left[(V_o + V_1)^{1/2} + V_o^{1/2}\right] . \qquad (12)$$

The available data are, t_1 = 1.2 microseconds for V_1 = 30 volts, t_2 = 1.4 microseconds for V_2 = 10 volts, and t_3 = 1.6 microseconds for V_3 = 5 volts. Using these data, we obtain V_o = 10 volts from Eq. (12), and $m/e = 57 \times 10^{-8}$ Kg/Coul. The m/e ratio for Ti is 50×10^{-8} Kg/Coul. This shows that we have 10 eV Ti ions coming out of the target. Such an energy must be much greater than the average ion-thermal energy.

The high-initial velocity of the ions can be accounted for by a blow-off phenomenon at the source point. The blow-off of the material occurs due to the high-initial density of the evaporated gas. That such is the case is evidenced by the presence of small craters created by the focused laser beam on the target surface.

A one dimensional blow-off is also known as a complete rarefaction wave.[8-9] The problem consists of an infinite shock tube divided into two parts by a membrane. The left half of the tube is filled with a gas, and the right half is a vacuum. At $t = 0$, the membrane is removed instantaneously, causing the gas to expand adiabatically into the vacuum space. The solutions of this problem are given by

$$\frac{\rho}{\rho_o} = \left\{1 - \left[\frac{(\gamma - 1)}{(\gamma + 1)}\right]\left[\frac{(x + c_o t)}{c_o t}\right]^{2/\gamma - 1}\right\} \tag{13}$$

and

$$\frac{u}{C_o} = \left[\frac{2}{(\gamma + 1)}\right]\left[\frac{(x + c_o t)}{c_o t}\right] . \tag{14}$$

ρ is the density, u is the flow velocity, c_o is the sound speed in the undisturbed gas, and $\gamma = 1 + (R/c_v)$ is the ratio of specific heats. Note that the disturbance propagates to the left at sound speed c_o, while the front layer of the gas moves towards the right at the "escaping speed" $u_e = 2c_o/(\gamma - 1) = 2c_v c_o/R$. For a monatomic gas at low densities and ordinary temperatures, $u_e/c_o = 3$. The corresponding value for a diatomic gas is 5. In the temperature range $T = 2000°K$ to $20,000°K$, the specific heat c_v can become as large as ten times the ordinary value due to excitation and ionization of molecules. Therefore, the ratio u_e/c_o can be as large as 30. This means that the front layer of the gas can attain a directed energy of more than ten times the thermal energy in the gas. If energy is continuously fed into the gas during the blow-off such as to make the process isothermal, then the escape speed approaches infinity.

In our experiment, the blow-off is three dimensional, with time dependent power input and with wall effects. A complete analysis of the processes is not only very difficult but also requires far more data than we have at hand. However, it is quite clear that the

blow-off mechanism can produce the high-energy particles observed in the experiment. Since the crater size is actually finite, the blow-off is essentially one dimensional at least at the first moment. By the time the blow-off loses its one dimensionality, an appreciable amount of gas would have already attained a high-directed energy. As the blow-off further develops, the directed energy of any gas element can only increase with time, no matter how complicated the blow-off becomes. As discussed in the preceding paragraph, this directed energy can well exceed the thermal energy of the gas. In experiment III, the highest directed energy per ion was found to be about 10 eV. This directed energy can be produced by a blow-off of a, say, 1 eV gas. In experiment V, each laser pulse produces two current pulses. The slower and larger of the two pulses is very similar to the current pulse observed in experiment III, both in shape and in time. This current is presumably induced by Ti^+ ions. At zero-bias voltage, its peak is delayed from the laser pulse by about 1.8 microseconds. This corresponds to Ti^+ ions with about 7 eV directed energy. The delay time decreases as the negative bias increases.

The faster and smaller of the two pulses is delayed from the laser pulse by about 0.4 microseconds, essentially independent of the bias voltage. This seems to indicate that the current is not caused by ions. The delay time is also too large to be accounted for by photoelectrons produced at the collector. One possible explanation is that the current is caused by secondary electrons produced at the collector by fast D_2 (neutral) particles. If this is the case, these D_2 particles must have a maximum directed energy of about 10 eV. Presumably, these D_2 particles are released from the target surface before the Ti base starts to evaporate. The high-directed energy can again be explained by the blow-off mechanism. Evaporation of the target leads to a second blow-off which is responsible for the slower pulse. The evaporated gas presumably

contains both titanium and deuterium particles. However, the ions are predominantly Ti^+, due to the significantly lower ionization potential of Ti.

G. DISCHARGE IN THE DIODE

When the collector was biased to over 21 volts, the focused giant pulse laser was found to trigger a gaseous discharge in the diode. The experimental data are summarized in Table II.

TABLE II

Bias	Current	Diode Voltage	Duration of Discharge
21 volts	1.85 amp	16.0 volts	7 microsec
22 volts	2.22 amp	16.0 volts	>12 microsec
25 volts	3.15 amp	16.5 volts	—
27 volts	3.33 amp	18.0 volts	—
30 volts	4.07 amp	19.0 volts	27 to 100

Note that the diode voltage (= bias - $IR_{external}$) is always above the ionization potential of D_2 (15.5 volts). This seems to indicate that the discharge is maintained by ionization of D_2 molecules. The titanium atoms with much lower ionization potential do not seem to contribute to the discharge, probably because they quickly condense out on cold surfaces.

V. SUMMARY OF OBSERVED FACTS

1. The work function of titanium is found to be lowered by about ten percent by the presence of a monolayer or by the occlusion of deuterium particles.

2. A nonfocused giant pulse laser beam produces a very uneven temperature distribution on the target surface. A few very small but very hot spots seem to emit electrons at 7000°K.

3. A 1000 time increase of the input power density causes only a two-fold increase in electron temperature. The temperature rise is presumably limited by a large specific heat at high temperatures and the increased transparency of the material due to expansion.

4. A focused giant pulse laser always induces a deuterium gas discharge in the diode when the collector bias is greater than 21 volts. Titanium particles do not seem to contribute to the discharge, presumably due to their fast condensation on cold surfaces.

5. The nonfocused giant pulse laser seems to excite direct emission of both Ti^+ and D_2^+ ions from the target surface. Space charge and collisional effects are insignificant in this case due to the low-ion densities.

6. A focused-laser beam can lift off up to 10^{15} neutrals and ions from the target surface. The very high pressure in the evaporated material leads to a blow-off phenomenon in the vacuum. Particles near the surface are accelerated to energies up to 10 eV by this mechanism. An appreciable number of titanium atoms are ionized in the gas and induces a current in the external circuit.

7. If the target is Ti-D, a focused giant pulse laser releases a large number of deuterium particles before evaporating the main body of the target. A blow-off also develops, which accelerates some D_2 particles to an energy of 10 eV. The current induced by this blow-off seems to be caused by secondary electrons produced at the collector by fast neutrals, rather than caused by ions. Degree of ionization in the D_2 gas is presumably inappreciable due to the relatively high-ionization potential.

VI. ACKNOWLEDGMENTS

The author is most grateful to Professor C. K. Birdsall for his encouragement and many valuable discussions. He also wants to thank Dr. S. A. Colgate who brought the blow-off mechanism to his attention. The experiment was suggested by Professor A. W. Trivelpiece. The Ti-D disk was prepared by J. Spector. The laser was borrowed from Professor J. Singer.

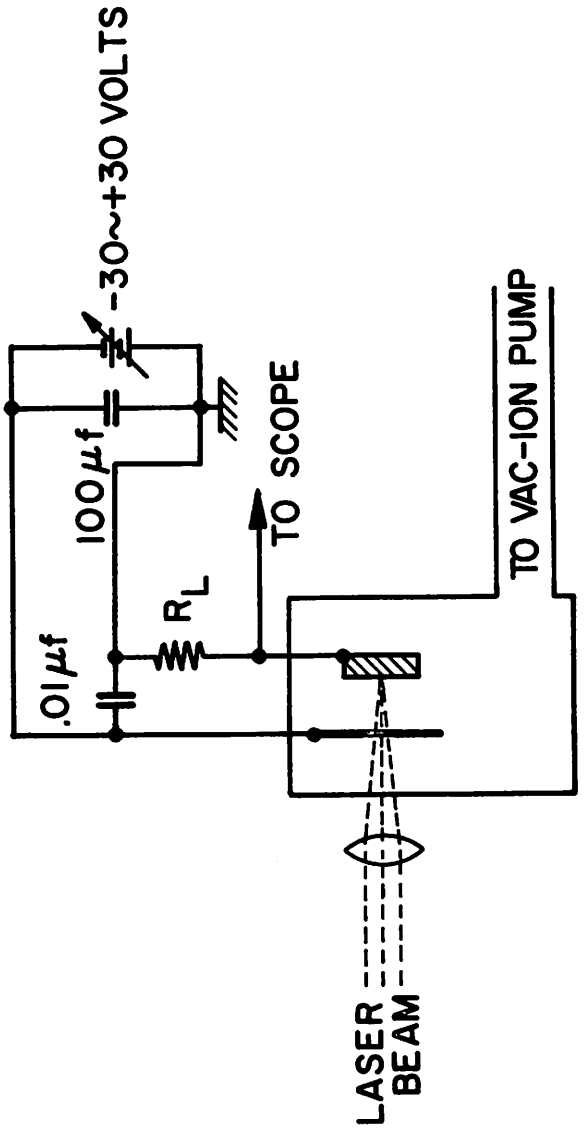

Fig. 1. Experimental arrangement.

M-84a

LASER INDUCED EMISSION OF ELECTRONS, IONS, AND NEUTRALS FROM Ti AND Ti-D SURFACES*

T. Y. CHANG AND C. K. BIRDSALL
Electronics Research Laboratory, Electrical Engineering Department
University of California, Berkeley, California

The plasma produced from deuterated titanium disks due to laser induced emission is described in this paper. The ion and electron pulses are similar to those described by others working with pure metals.[1-7] Three additional points are put forth to make the observations consistent with calculations; (i) the measured electron temperature at low laser intensity far exceeds the calculated surface temperature, implying non-uniform emission, primarily from small hot spots; (ii) the ion pulses at low laser intensity are double-peaked with the peaks truly representing D_2^+ and Ti^+ transit times consistent with calculations assuming zero initial energies; (iii) pulses at high laser intensity require assuming nonzero initial energies for consistency. A blow-off mechanism is postulated as responsible for the production of ions with high initial energies; some justification is given for this. The fast pulse (similar to "reverse photoelectric effect" of Ref. 2) is postulated as due to fast neutral atoms from the blow-off causing electron emission at the anode.

The experimental apparatus consists of a vacuum diode with a circular window on the collector. The laser is rated at 1-joule output. The vacuum is maintained at 10^{-7} Torr. The Ti-D disc is loaded with about 1 D atom to 2 Ti atoms. The bias voltage was varied from -30 volts to +30 volts; the load resistor was varied from 10^5 ohms to 2.7 ohms depending on the current. The relative intensity of the laser beam was monitored by a photo tube, picking up the light scattered from the surface of the focusing lens.

Three experiments are summarized in Table I. The laser spot size was obtained from the size of the craters created by the heating,

*The research herein was supported by the Joint Services Electronics Program (Air Force Office of Scientific Research, Army Research Office, Office of Naval Research) under Grant AF-AFOSR-139-63/139-64.

measured in experiments II and III. The temperature rises shown are calculated from surface heating of titanium only to give a rough estimate of the temperature at the end of one microsecond.

In our experiments the electron emission appears to be due primarily to thermionic emission. From plots of electron emission as a function of retarding potential, an electron temperature of 7000 °K was found for experiment I. This temperature is very high compared with the apparent surface temperature given in Table I; this is also incompatible with the small emission current. These two facts imply that the temperature distribution on the target surface is extremely peaked at one or more small spots. Because of the nonlinearity of the emission (Richardson) equation with temperature, the electrons will come almost exclusively from these hottest spots. In experiment III, where the laser is focused, the calculated surface temperature is increased by 10^3, but the electron temperature determined from a retarding potential plot is only 16,600 °K, about twice the value in experiment I. This small rise is presumably due to a large increase in specific heat at high temperature and the increased transparency of the material due to large expansion of the heated surface. For positive collector bias greater than 21 volts, the focused giant pulse laser always triggers a gaseous discharge in the diode.

Information about ion current that can be gained from the experiment is from the pulse shape of the ion current as induced in the external circuit. A prime question is correlation of the ion transit time (to measure energy) with the peak of ion current. In experiment I, which used Q-switched but not focused light, the charge density and current were low, allowing us to neglect collisions and changes of potential in the diode due to the space charge and IR drop in the circuit. The ion thermal energies are taken to be small compared to the potential energy across the diode and the ions are assumed to be emitted with zero initial velocity at the target surface. The ion current at the target is taken to decay exponentially with time with an e-folding time of 4 microseconds as determined from the tail of the actual ion current pulses. By combining these assumptions with the equation of continuity, and the equation of motion, the D_2^+ ion current is

found to follow the following law at position x as a function of time.

$$J_D = J_{Do} \exp \left[(1/\tau)(2 m_D x/eE)^{1/2} - (t/\tau)\right] . \qquad (1)$$

The current induced in the diode can be obtained from power balance. For early times, $0 < t < t_D$, where t_D is the transit time for a D_2^+ ion, the diode is partially filled with ions and the induced current has the following behavior with time:

$$I_D = 2J_{Do}(\tau / t_D)^2 \left[\exp(-t/\tau) - 1 + (t/\tau)\right] . \qquad (2)$$

For times greater than t_D, the induced current is given by Eq. (3),

$$I_D = 2J_{Do}(\tau / t_D)^2 \left[1 - (1 - (t_D/\tau)) \exp (t_D/\tau)\right] \exp(-t/\tau) . \qquad (3)$$

With both D_2^+ and Ti^+ ions emitted, the currents must be added. A typical result would be as sketched in Fig. 1a. This result is in good agreement with the form of the experimental pulse shown in Fig. 1b.

However, for the more intense radiation, experiments II and III, we have to allow for a nonzero initial velocity for the ions. By using different biases and observing the different delay times to the peaks of ion currents, we can solve for the initial energy and M/e of ions. We find an initial energy of 10 eV volts and Me $\cong 57 \times 10^{-8}$ kg/coulomb in experiment II. M/e ratio for Ti is 50×10^{-8}, implying Ti^+ ions. Such an energy must be much greater than the average ion-thermal energy.

The high initial velocity of the ion may be accounted for by a blow-off of the rapidly expanding high density gas. The small craters created by the focused laser give evidence of this phenomenon. The one-dimensional blow-off, or complete rarefaction wave, has been treated by Courant and Friedrichs[8] and Lelevier;[9] their work will be used to estimate the front velocity. When a gas is suddenly allowed to expand into a vacuum, the disturbance propagates into the gas at sound speed c_o, while the front of the gas moves into the vacuum at escape speed u_e given by

$$u_e = 2 c_o/(\gamma - 1) = 2 c_v c_o/R . \qquad (4)$$

γ is the ratio of specific heats. c_v is the specific heat of the gas at constant volume. R is the gas constant. In a temperature range of $T = 2000^{\circ}K$ to $20,000^{\circ}K$, the specific heat c_v can become as large as ten times the ordinary value due to excitation and ionization of the molecules. Thus the ratio of u_b/c_o which is 3 to 5 at low temperatures, can become as large as 30. This means that a leV gas can produce ions with escape energy of 10eV. If energy is continually fed into the gas during the blow-off, such as to make the process isothermal, then the escape speed approaches infinity.

In our experiments, the blow-off is three-dimensional with time dependent power input and wall effects. A complete analysis of the process is not only very difficult but also requires far more data than we have at hand. However, it is quite clear that the blow-off mechanism can produce the high energy particles observed in the experiment. Since the crater size is actually finite, the blow-off is essentially one-dimensional, at least at the first moment. By the time the blow-off loses its one dimensionality, an appreciable amount of gas would have attained a high directed energy. As the blow-off further develops, the directed energy of any gas element can only increase with time, no matter how complicated the blow-off becomes.

In experiment III, each laser pulse produces two current pulses as shown in Fig. 2. The slower and larger of the two pulses is very similar to the current pulse observed in experiment II, both in shape and in time. This current is presumably induced by Ti + ions. At zero bias voltage, its peak is delayed from the laser pulse by about 1.8 microseconds. This corresponds to Ti^+ ions with about 7 eV directed energy. The delay decreases as the negative bias increases. The faster and smaller of the two pulses is delayed from the laser pulse by about 0.4 microsecond, essentially independent of the bias voltage. [Similar pulses have been seen by others, called "reverse photoelectric effect" by Ready.[2]] This seems to indicate that the current is not caused by ions. The delay time is also too large to be accounted for by photoelectrons produced at the collector. One possible explanation is that the current is caused by secondary

electrons produced at the collector by fast D_2 (neutral) particles. If this is the case, these D_2 particles must have a maximum directed energy of about 10 eV. Presumably these D_2 particles are released from the target surface before the Ti base starts to evaporate. The high directed energy can again be explained by the blow-off mechanism. Evaporation of the target leads to a second blow-off which is responsible for the slower pulse. The evaporated gas presumably contains both titanium and deuterium particles. However, the ions are predominantly Ti^+ due to the significantly lower ionization potential of Ti.

ACKNOWLEDGMENT

We are indebted to Dr. A. W. Trivelpiece, who suggested the experiment; J. Spector, who prepared the Ti-D disk; Dr. J. Singer, who lent us his laser unit; and Dr. S. A. Colgate, who suggested the blow-off mechanism.

REFERENCES

1. R. E. Honig and J. R. Woolston, "Laser-induced emission of electrons, ions, and neutral atoms from solid surfaces," Appl. Phys. Letters 2, 138 (1963).

2. D. Lichtman and J. F. Ready, "Laser beam induced electron emission," Phys. Rev. Letters 10 342 (1963).

3. R. E. Honig, "Laser-induced emission of electrons and positive ions from metals and semiconductors," Appl. Phys. Letters 3, 8 (1963).

4. J. F. Ready, "Development of plume of material vaporized by giant pulse lasers," Appl. Phys. Letters 3, 11 (1963).

5. D. Lichtman and J. F. Ready, "Reverse photo-electric effect and positive ion emission caused by Nd-in-glass laser radiation," Appl. Phys. Letters 3, 115 (1963).

6. G. C. Dalman and L. A. MacKenzie, "Invesitgation of new concepts for microwave power generation (laser studies)," Rome Air Development Center RADC-TDR-63-465, II (1963).

7. W. I. Linlor, "Ion energies produced by laser giant pulse," Appl. Phys. Letters 3, 210 (1963).

8. R. Courant and K. O. Friedrichs, "Supersonic flow and shock waves," Interscience (1948).

9. R. Lelevier, "Lectures on hydrodynamics and shock waves," Univ. of Calif. Radiation Lab.-4333 (1954).

TABLE I

Experiment	I	II	III
Target	Ti-D	Ti	Ti-D
Laser type	Q-switched	non-Q-switched	Q-switched
power(Kw)	~ 100	~ 10	~ 100
spot size (cm^2)	~ 0.3	$\sim 10^{-3}$	$\sim 10^{-3}$
pwr density (w/cm^2)	$\sim 10^5$	$\sim 10^7$	$\sim 10^8$
Bias(volts)		peak electron current	
30	--	100→3μA	4.5A;discharge
20	--	--	3.3A
12	--	--	2.4A
0	0.8μA	--	0.40A
-2	0.2μA	--	0.25A
		peak ion current	
0	0	--	0.02A
-3	0.7μA(-4v)	--	0.15A
-30	--	10→0.5μA	5.6A
Electrons collected per pulse	1.1×10^7 w. no bias	--	1.5×10^{13} w. 10v. bias
Ions collected	2.3×10^7 w. -4v. bias	--	6.3×10^{13} w. -30v. bias
T_e(°K) from retarding potential plot	7,000		16,600
Calculated temperature rise from heat flow equation			
$T-T_o$(°K)	34	3400	34000

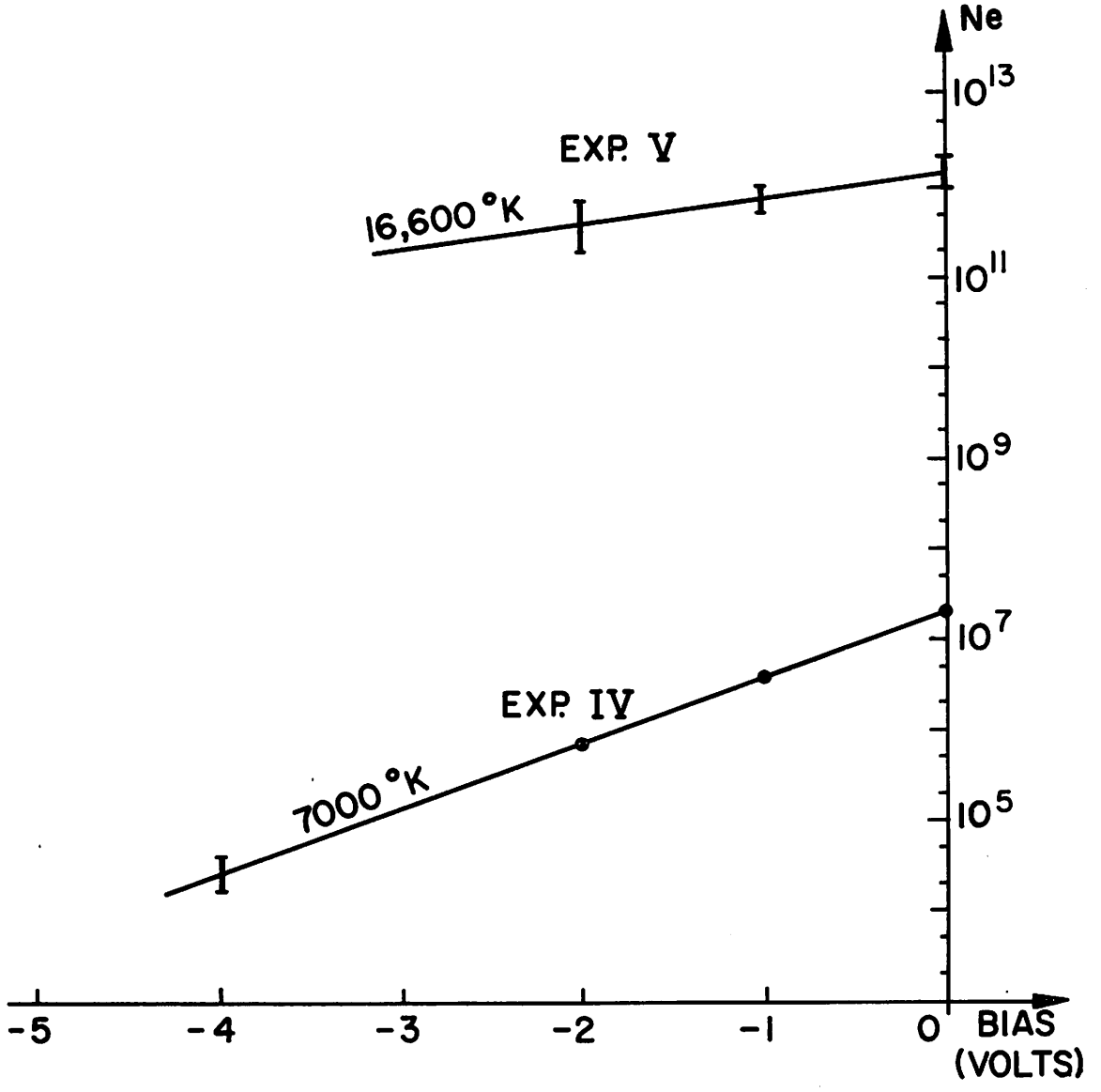

Fig. 2. Number of electrons collected per pulse.

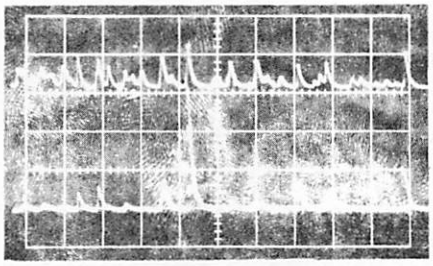

Fig. 3. Experiment I
collector bias: 30 v
time scale: 20 usec/major div.
upper trace: laser output
lower trace: electron current
10 uamp/major div.

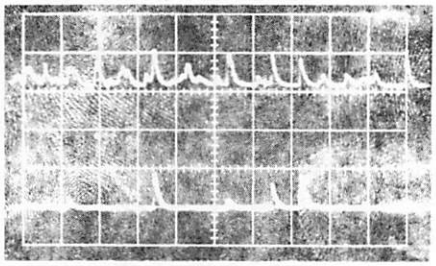

Fig. 4. Experiment I
collector bias: 10 v
time scale : 20 usec/major div.
upper trace: laser output
lower trace: electron current
10 uamp/major div.

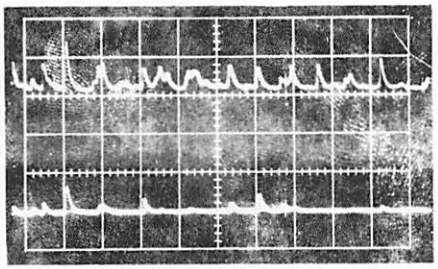

Fig. 5. Experiment I
collector bias: 0 v
time scale: 20 usec/major div.
upper trace: laser output
lower trace: electron current
10 uamp/major div.

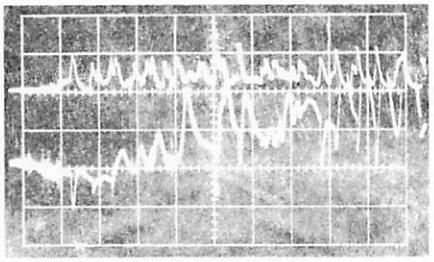

Fig. 6. Experiment I
collector bias: - 2 v
time scale: 20 usec/major div.
upper trace: laser output
lower trace: ion current
0.5 uamp/major div.

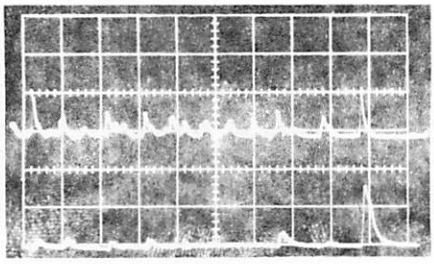

Fig. 7. Experiment I
collector bias: - 3 v
time scale: 20 usec/major div.
upper trace: laser output
lower trace: ion current
0.5 uamp/major div.

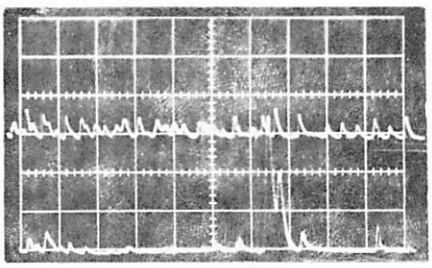

Fig. 8. Experiment I
collector bias: - 30 v
time scale: 20 usec/major div.
upper trace: laser output
lower trace: ion current
0.5 uamp/major div.

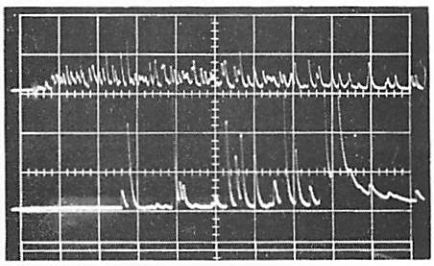

Fig. 9. Experiment II
collector bias: 30 v
time scale: 40 usec/major div.
upper trace: laser output
lower trace: electron current
10 uamp/major div.

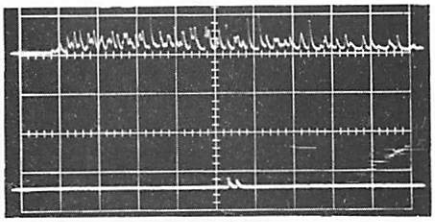

Fig. 10. Experiment II
collector bias: 30 v
time scale: 40 usec/major div.
upper trace: laser output
lower trace: electron current*
10 uamp/major div.

* After repeated bombardments.

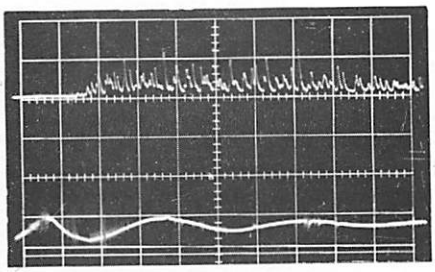

Fig. 11. Experiment II
collector bias: - 30 v
time scale: 40 usec/major div.
upper trace: laser output
lower trace: ion current*
0.5 uamp/major div.

* Only the external disturbance is seen.

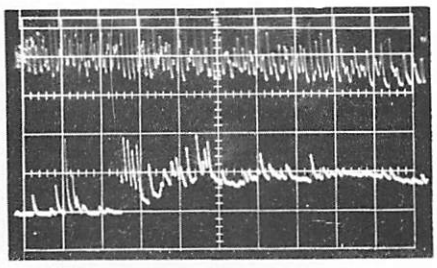

Fig. 12. Experiment III
collector bias: 30 v
time scale: 40 usec/major div.
upper trace: laser output
lower trace: electron current
50 uamp/major div.

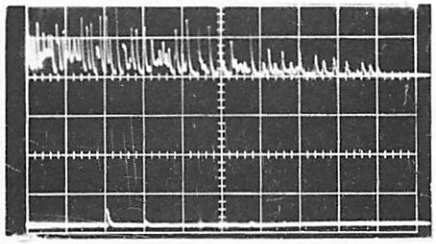

Fig. 13. Experiment III
collector bias: 30 v
time scale: 50 usec/major div.
upper trace: laser output
lower trace: electron current*
10 uamp/major div.

* After repeated bombardments.

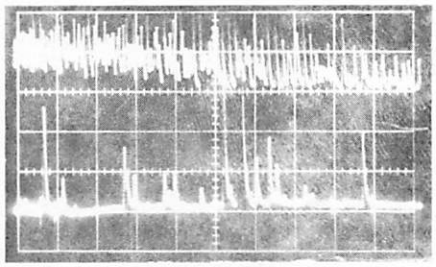

Fig. 14. Experiment III
collector bias: - 30 v
time scale: 50 usec/major div.
upper trace: laser output
lower trace: ion current
1 uamp/major div.

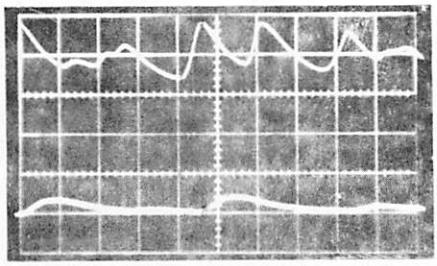

Fig. 15. Experiment III
collector bias: - 30 v
time scale 2 usec/major div.
upper trace: laser output
lower trace: ion current
1 uamp/major div.

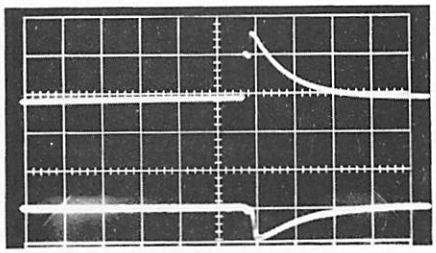

Fig. 16. Experiment IV
collector bias: 0 v
time scale: 2 usec/major div.
upper trace: laser output
lower trace: ion current
1 uamp/major div.

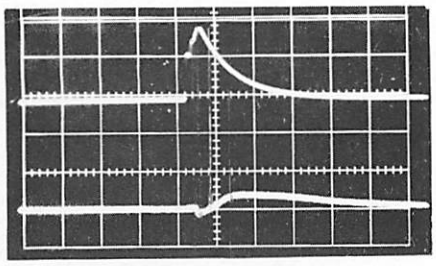

Fig. 17. Experiment IV
collector bias: - 2 v
time scale: 2 usec/major div.
upper trace: laser output
lower trace: ion current
1 uamp/major div.

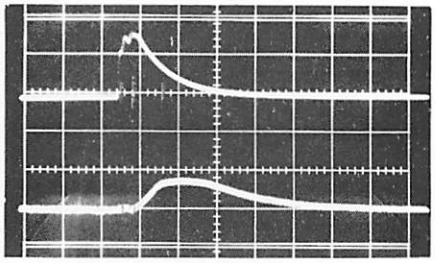

Fig. 18. **Experiment IV**
collector bias: - 4 v
time scale: 2 usec/major div.
upper trace: laser output
lower trace: ion current
1 uamp/major div.

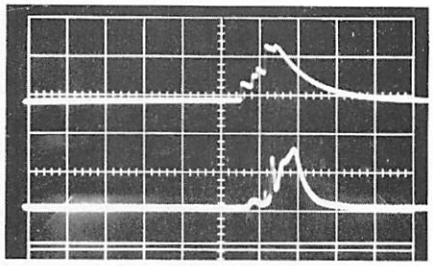

Fig. 19. Experiment V
collector bias: - 30 v
time scale: 2 usec/major div.
upper trace: laser output
lower trace: ion current
3. 7 amp/major div.

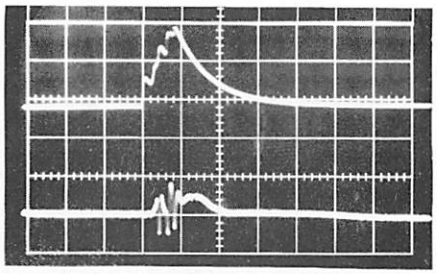

Fig. 20. Experiment V
collector bias: - 3 v
time scale: 2 usec/major div.
upper trace: laser output
lower trace: ion current
0. 37 amp/major div.

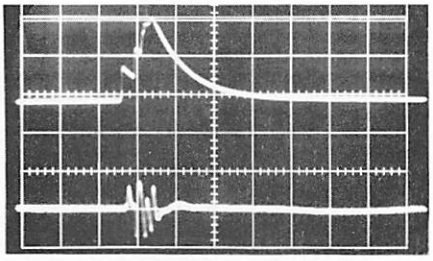

Fig. 21. Experiment V
collector bias: - 2 v
time scale: 2 usec/major div.
upper trace: laser output
lower trace: ion current
0. 37 amp/major div.

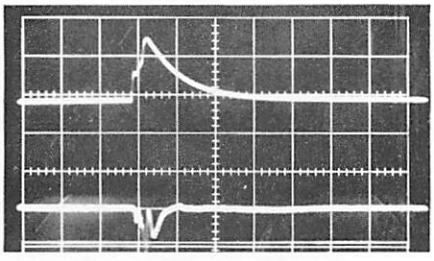

Fig. 22. Experiment V
collector bias: 0 v
time scale: 2 usec/major div.
upper trace: laser output
lower trace: ion current
0. 37 amp/major div.

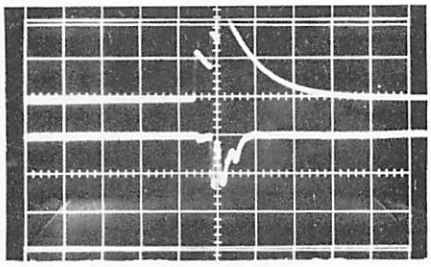

Fig. 23. Experiment V
collector bias: 12 v
time scale: 2 usec/major div.
upper trace: laser output
lower trace: ion current
1.85 amp/major div.

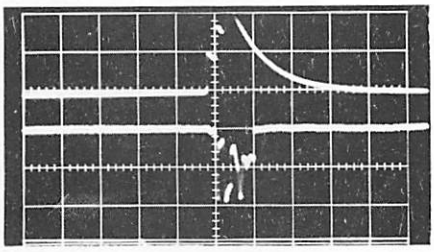

Fig. 24. Experiment V
collector bias: 20 v
time scale: 2 usec/major div.
upper trace: laser output
lower trace: ion current
1.85 amp/major div.

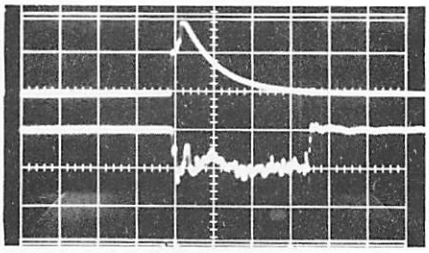

Fig. 25. Experiment V
collector bias: 21 v
time scale: 2 usec/major div.
upper trace: laser output
lower trace: ion current
1.85 amp/major div.

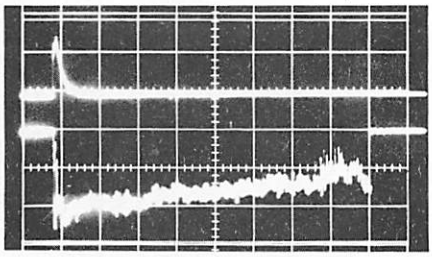

Fig. 26. Experiment V
collector bias: 30 v
time scale: 10 usec/major div.
upper trace: laser output
lower trace: ion current
1.85 amp/major div.

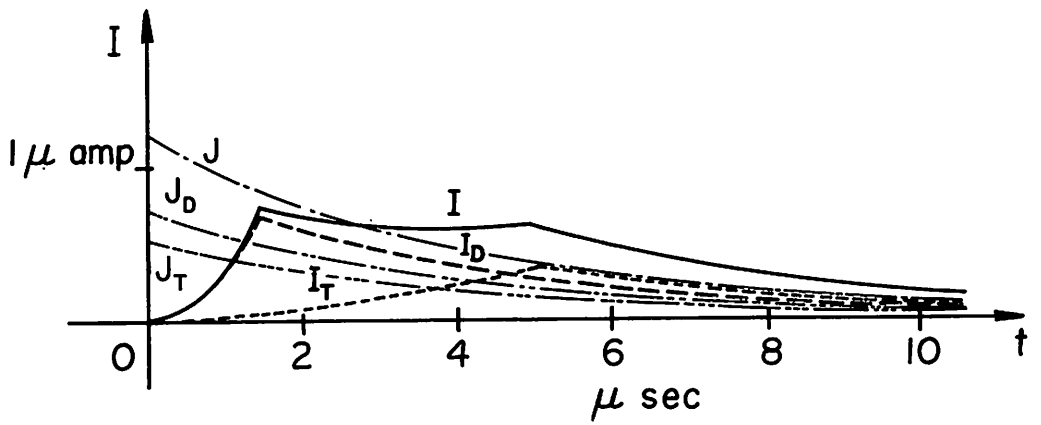

Fig. 27. Ion currents for v = 4.0 volts, τ = 4.0 μsec
J_{D_o} = 0.7 μamp., J_{T_o} = 0.5 μamp.

REFERENCES

1. R. E. Honig and J. R. Woolston, "Laser-induced emission of electrons, ions, and neutral atoms from solid surfaces," Appl. Phys. Letters 2, 138 (1963).
2. D. Lichtman and J. F. Ready, "Laser beam induced electron emission," Phys. Rev. Letters 10, 342 (1963).
3. R. E. Honig, "Laser-induced emission of electrons and positive ions from metals and semiconductors," Appl. Phys. Letters 3, 8 (1963).
4. J. F. Ready, "Development of plume of material vaporized by giant pulse laser," Appl. Phys. Letters 3, 11 (1963).
5. D. Lichtman and J. F. Ready, "Reverse photo-electric effect and positive ion emission caused by Nd-in-glass laser radiation," Appl. Phys. Letters 3, 115 (1963).
6. G. C. Dalman and L. A. MacKenzie, "Investigation of new concepts for microwave power generation (laser studies)," Rome Air Development Center RADC-TDR-63-465, II, (1963).
7. W. I. Linlor, "Ion energies produced by laser giant pulse," Appl. Phys. Letters 3, 210 (1963).
8. R. Courant and K. O. Friedrichs, "Supersonic flow and shock waves," Interscience (1948).
9. R. Lelevier, "Lectures on hydrodynamics and shock waves," Univ. of Calif. Radiation Laboratory-4333 (1954).